Automated velocity mapping of migrating cell populations (AVeMap)

Maxime Déforet, Maria Carla Parrini, Laurence Petitjean, Marco Biondini, Axel Buguin, Jacques Camonis, Pascal Silberzan

Automated velocity mapping of migrating cell populations (AVeMap)

Maxime Deforet[1,3], Maria Carla Parrini[2,3], Laurence Petitjean[1], Marco Biondini[2], Axel Buguin[1], Jacques Camonis[2] & Pascal Silberzan[1]

Characterizing the migration of a population of cells remains laborious and somewhat subjective. Advances in genetics and robotics allow researchers to perform many experiments in parallel, but analyzing the large sets of data remains a bottleneck. Here we describe a rapid, fully automated correlation-based method for cell migration analysis, compatible with standard video microscopy. This method allows for the computation of quantitative migration parameters via an extensive dynamic mapping of cell displacements.

The wound-healing assay[1] is the technique of choice for studying the impact of large collections of siRNAs[2,3] or drugs[4] on the migration of cell populations[1,5]. The wound area can be dynamically monitored in an automated way[6,7], but characterizing higher-resolution migration features such as velocity or persistence generally involves the manual tracking of individual cells from movies. This is a time-consuming procedure that limits *de facto* the amount of information that can be processed. Moreover, cell tracking is notoriously prone to errors because it is repetitive, laborious, operator dependent and influenced by the subjective choice of cells to track[8]. Strategies relying on automated tracking considerably improve the amount and quality of tractable data in low-density monolayers[8,9] or when using fluorescently labeled cells[3]; however, their use is restricted to these particular situations. To analyze the migration of unlabeled confluent monolayers, we describe a fully automated whole-field technique based on a different mode of data analysis.

We and others have previously applied image correlation techniques as alternatives to tracking for the analysis of collective movements of cells in monolayers from phase-contrast video-microscopy movies[10,11]. Here we describe user-friendly software for fast and automated extraction of quantitative parameters describing monolayers of migrating cells (**Supplementary Software**). Our method and the corresponding software—coined AVeMap for 'automated velocity mapping of migrating cell populations'—are based on the particle image velocimetry (PIV) technique[12,13] that consists of dynamically mapping the velocity field within the monolayer via local correlations between successive images (**Supplementary Fig. 1**).

AVeMap can analyze in parallel a large number of phase-contrast time-lapse videos of cells migrating after wounding (**Fig. 1**). We compared AVeMap and manual cell tracking by analyzing the migration of HEK-HT[14] cells with each technique. Cells were transfected with siRNA against luciferase (siLuc, control) or Wave2 (siWave2, Wave2-depleted cells), a component of the WAVE complex that is required for cell migration[15] (**Fig. 2a** and **Supplementary Fig. 2**). Both migrating monolayers kept their integrity (**Supplementary Videos 1** and **2**).

Because of the high cell density in the monolayer, manual cell tracking can be used only for the cells at the edges. In contrast, because AVeMap relies on local correlations between images, it can measure displacements within the monolayer. AVeMap analyzes a strip of cells from the edge of the monolayer whose width is adjustable by the user. For comparison with cell tracking, the width was chosen here to be 50 μm (the approximate size of an HEK-HT cell at the edge) (**Supplementary Fig. 3**).

Cell tracking measures both velocity (V) and persistence (P) for the first cell row. The instantaneous local velocity is defined as the ratio of the cell displacement between successive images to the time interval. P is the end-to-end distance of a cell trajectory divided by its total length (**Supplementary Fig. 4**). AVeMap measures the velocity of all border cells and computes an order parameter, $S = \langle \cos \theta \rangle$ (**Fig. 1** and **Supplementary Fig. 4**), where θ is the angle between the local velocity and the normal to the average direction of the border and angle brackets '$\langle \ldots \rangle$' denote a spatial averaging. Cells migrating perfectly perpendicularly to the edge are characterized by $S = 1$, whereas cells migrating randomly are characterized by $S = 0$. P and S are not identical, but they are each a measure of the angular deviation from an oriented straight-line progression (**Supplementary Discussion 1**).

AVeMap yields velocities systematically smaller than does manual tracking (**Fig. 2b** and **Supplementary Fig. 2**), mainly because of the overestimation introduced by manually pointing and clicking on cells[8] (**Supplementary Fig. 5**). However, both techniques report that depletion of Wave2 results in a substantial decrease in migration velocity (**Fig. 2b**) and a stronger decrease of P and S (**Fig. 2c** and **Supplementary Fig. 6**), indicating that a loss of directionality is the primary cause of the dramatic alteration of the wound closure caused by Wave2 depletion (**Fig. 2a**). Furthermore, virtual trajectories reconstructed from the AVeMap velocity field are very close to the manually determined trajectories (**Supplementary Discussion 2**). AVeMap is therefore a
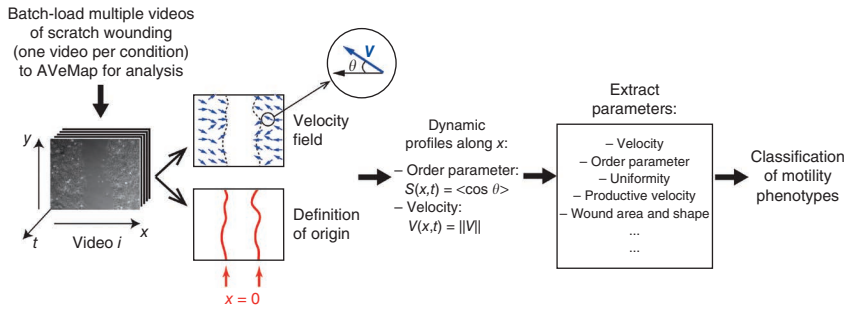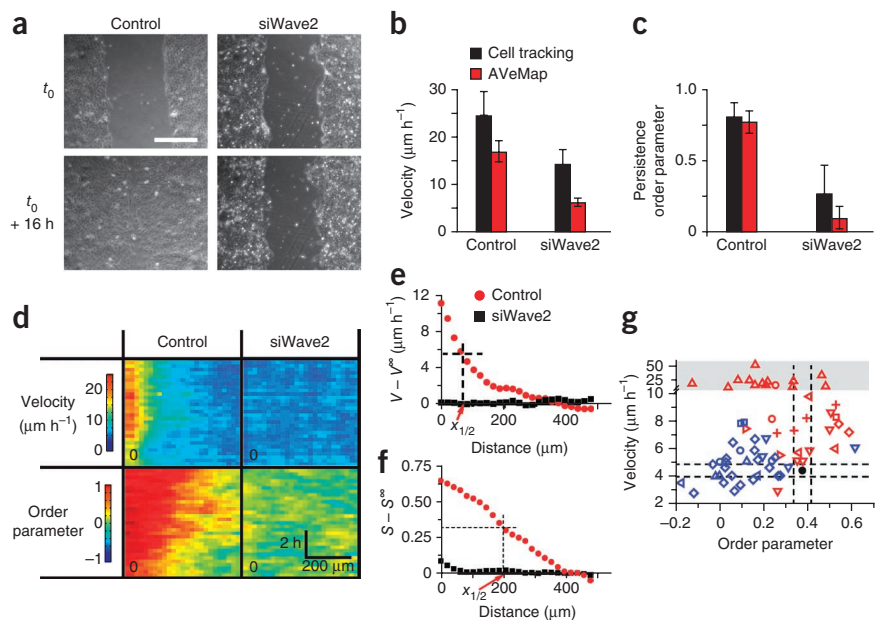
Figure 1 | Schematic of AVeMap. Multiple videos of cell migration (such as in a wound-healing assay) are analyzed by AVeMap. For each frame of a given video, the software computes (i) the local velocities (velocity field), using correlations between successive images, and (ii) the monolayer edges that locally define the origin of the x axis. For each video, the velocity and the order parameter are analyzed in time and space to extract quantitative parameters characterizing the cell motility phenotype. The different conditions (videos) can then be classified according to these parameters.

reliable alternative to manual tracking for characterizing migration features, but it is automated and can perform within dense populations of cells. Of note, a weaker depletion of Wave2 led to intermediate values of V and S (**Supplementary Fig. 7** and **Supplementary Video 3**), whereas treatment with transforming growth factor β yielded a larger V and a smaller S on A549 cells compared to control (**Supplementary Fig. 7** and **Supplementary Videos 4** and **5**).

After about 3 h, the displacements at the edge of the control monolayer were faster and more directed than those within the monolayer (**Fig. 2d–f**)[10,16]. The software quantifies these gradients by the distance $x_{1/2}$ it takes for the edge values of V and S to be divided by 2. For users interested in mapping the cell behaviors in deeper layers, full spatiotemporal heat maps (**Fig. 2d**) can be generated from the AVeMap analysis by using the complementary software AVeMap+.

Finally, we have applied AVeMap to data from a previously published siRNA screen aimed at identifying genes regulating MCF-10A epithelial cell migration[2]. In the original work, a high-throughput end-point wound-healing screen identified 66 genes whose silencing significantly affected migration; the associated migration features were then characterized by manual cell tracking. We have analyzed with AVeMap the same 67 movies (66 + control) used in this latter analysis.

The productive velocity, $V_P = V \times S$, is clearly correlated with wound closure speed (**Supplementary Fig. 8**), and classification of the genes based on V_P largely overlapped the 'impaired' and 'accelerated' classifications in ref. 2 (**Supplementary Fig. 9**) with a few exceptions that would be worthwhile revisiting (**Supplementary Table 1**). We observed that impaired wound closure corresponds to small S values, whereas accelerated migration is correlated with a large velocity (**Fig. 2g**). AVeMap therefore allows genes to be clustered on the basis of objective and quantitative measurements (V and S) (**Fig. 2g** and **Supplementary Table 1**). We note that the analysis time of a typical cell-migration movie (20 h, 500 × 500–pixel images shot every 15 min) is only 2 min. Consequently a duplicate genome-wide screen (using pools of siRNA for 20,000 genes) would require an analysis time of ~56 d, or less than a week if dispatched over ten computers, making possible large-scale video-microscopy screens of cell migration. With minor modifications of the source code, the AVeMap interface can be used in other situations such as embryonic morphogenesis[12].

Figure 2 | AVeMap analysis of migrating monolayers. (**a**) Micrographs show HEK-HT monolayers at the indicated time points after wounding for control and Wave2-depleted cells (siWave2). Scale bar, 500 µm. (**b,c**) Analysis of velocity (**b**) and directionality (**c**) of migrating HEK-HT monolayers as in **a** by manual cell tracking and AVeMap (performed on the first cell row). Error bars, s.d. ($n = 32$ for cell tracking; $n = 40$ for AVeMap). (**d**) Heat maps show spatiotemporal evolution of the velocity V and the order parameter S for the control and siWave2-treated cells (vertical axis, time; horizontal axis, distance from edge). Each row corresponds to an average over the vertical direction (y axis in **Fig. 1**). The point 0 is the origin on both axes. The data used for these graphs were generated with the AVeMap+ add-on. (**e,f**) Plots showing time-averaged profiles of velocity V (**e**) and order parameter S (**f**) along the x axis ($t > 3$ h). V^∞ and S^∞ are the values of these two parameters far from the leading edge. (**g**) AVeMap analysis of videos from a previous siRNA screen for genes involved in MCF-10A cell migration[2]. Velocity is plotted versus order parameter, and each point corresponds to one gene (**Supplementary Table 1**). Blue symbols, impaired motion; red symbols, accelerated motion, as defined by ref. 2; solid black circle, control. Symbol shapes correspond to the phenotypic classes identified in ref. 2 (**Supplementary Table 1**). The dashed lines delineate a 10% deviation from the control in both directions. The high-velocity region (gray area; note the change in vertical scale) corresponds to cells dissociating from the monolayer.

METHODS

Methods and any associated references are available in the online version of the paper.

Note: Supplementary information is available in the online version of the paper.

AUTHORS CONTRIBUTIONS

M.D., L.P. and A.B. adapted the PIV technique to cell migration and developed the software. M.C.P. and M.B. performed the migration experiments and the cell tracking. All authors participated in the comparison of the two techniques. J.C. and P.S. conceived and supervised the project (equal contributions). All authors participated in the writing of the manuscript.

COMPETING FINANCIAL INTERESTS

The authors declare no competing financial interests.

1. Liang, C.-C., Park, A.Y. & Guan, J.-L. *Nat. Protoc.* **2**, 329–333 (2007).
2. Simpson, K.J. *et al. Nat. Cell Biol.* **10**, 1027–1038 (2008).
3. Vitorino, P. & Meyer, T. *Genes Dev.* **22**, 3268–3281 (2008).
4. Yarrow, J.C., Perlman, Z.E., Westwood, N.J. & Mitchison, T.J. *BMC Biotechnol.* **4**, 21 (2004).
5. Ridley, A.J. *et al. Science* **302**, 1704–1709 (2003).
6. Bai, S.W. *et al. BMC Biol.* **9**, 54 (2011).
7. Zaritsky, A. *et al. PLoS ONE* **6**, e27593 (2011).
8. Huth, J. *et al. BMC Cell Biol.* **11**, 24 (2010).
9. Hand, A.J., Sun, T., Barber, D.C., Hose, D.R. & MacNeil, S. *J. Microsc.* **234**, 62–79 (2009).
10. Petitjean, L. *et al. Biophys. J.* **98**, 1790–1800 (2010).
11. Angelini, T.E. *et al. Proc. Natl. Acad. Sci. USA* **108**, 4714–4719 (2011).
12. Supatto, W. *et al. Proc. Natl. Acad. Sci. USA* **102**, 1047–1052 (2005).
13. Raffel, M., Willert, C.E. & Kompenhans, J. *Particle Image Velocimetry: A Practical Guide* (Springer, Berlin, 1998).
14. Hamad, N.M. *et al. Genes Dev.* **16**, 2045–2057 (2002).
15. Takenawa, T. & Suetsugu, S. *Nat. Rev. Mol. Cell Biol.* **8**, 37–48 (2007).
16. Farooqui, R. & Fenteany, G. *J. Cell Sci.* **118**, 51–63 (2005).

ONLINE METHODS

Software availability. AVeMap was developed under MATLAB (MathWorks). It is available as an executable, multiplatform program, together with source codes and documentation at http://umr168.curie.fr/en/avemap, and the source code is also available as **Supplementary Software**. For practical reasons, this executable version, which does not require MATLAB, runs on a single processor. For users who want to customize the software and/or need the power of parallel computing, an installation of MATLAB with its 'parallel' and 'image processing' toolboxes is needed. Note that, even with the executable version, the velocity fields are stored for further analysis. The add-on AVeMap+ uses these AVeMap-computed velocity fields to generate heat map tables. It is available with the same link.

Wound-healing assays and image acquisition. Most of the experiments were performed on the HEK-HT cell line: human embryonic kidney cells stably expressing T/t antigens from SV40 and the catalytic subunit of telomerase hTERT[17].

Cells were grown in Dulbecco's modified Eagle's medium supplemented with 2 mM glutamine, antibiotics (penicillin and streptomycin) and 10% fetal bovine serum. Transient siRNA transfections were carried out with Hiperfect (Qiagen) according to manufacturer instructions; unless otherwise noted, final siRNA concentration was 5 nM. Targeted sequences were siLuc, CGTACGCGGAATACTTCGA; siWave2, AGTCACTCAGCTGGATCCC.

The depletion of Wave2 was verified by western blot using anti-Wave2 rabbit polyclonal antibody at 1:1,000 dilution (**Supplementary Fig. 2**).

A549 (adenocarcinoma human alveolar) cells[18] were grown in RPMI 1640 GlutaMAX (Invitrogen) supplemented with antibiotics (penicillin and streptomycin), 1 mM sodium pyruvate, 2.5 mg mL^{-1} d-glucose and 10% fetal bovine serum. Subconfluent cells were treated with 10 ng mL^{-1} human recombinant TGF-β1 (R&D #240-B) in complete culture medium for 4 d before the wound-healing assay. TGF-β1 treatment was maintained during the wound closure.

For wound-healing assays, cells were grown to confluence on 12-well dishes coated with collagen (type I from rat tail, Interchim 207050357, 120 μg mL^{-1} in H$_2$O for ≥1 h at 37 °C). The confluent monolayers were wounded with a pipette tip.

Starting from ≥3 h post-wounding, the cells were imaged on a Leica DMIRE2 inverted microscope equipped with a motorized stage for multipositioning, a CoolSNAP HQ2 camera (Roper Scientific) and a 'Box' heated chamber and 'Brick' CO$_2$ controller (Life Imaging Services) maintaining the 5% CO$_2$, humidified atmosphere and 37 °C culture conditions. This equipment was under control of the MetaMorph software (Universal Imaging). A phase-contrast 5× objective was used. Images (black and white, 8-bit) were acquired every 15 min, saved as .tiff files and compiled in stacks (one stack = one video) by MetaMorph. The resolution of each image was 1,300 × 1,030 pixels.

Note that for PIV analysis, it is important (i) to use low-magnification objectives to include in the field the cells far from the wound, (ii) to make the wounds reasonably vertical and (iii) to keep constant the illumination, the exposure time and all the camera acquisition parameters (for example, an auto-exposure option should not be used).

Manual cell tracking. For manual cell tracking analysis we used the Manual Tracking plug-in (http://rsb.info.nih.gov/ij/plugins/track/track.html, developed by F. Cordelières) of ImageJ software[19]. The displacements of 32 cells per video were followed for 5–8.5 h (20–34 time points of 15 min) by pointing the computer mouse at their nuclei at each time point and clicking on the center as determined visually. Data were exported to Microsoft Excel for mathematical and statistical analysis. To minimize any potential bias due to cell subset selection, the cells were randomly chosen by dividing each side of the wound into 16 segments and tracking one cell per segment to analyze 16 cells on the left side and 16 cells on the right side of the wound. However, in several cases, the cells initially selected could not be used over the whole experiment and had to be replaced by other ones for a variety of reasons: either they divided during the course of the experiment, their trajectories were lost, their nuclei were not visible or they went outside of the observation field.

AVeMap analysis. The software requires TIFF stacks or multi-image TIFF files that are to be uploaded before analysis. Note that uploading of the videos can be performed in parallel to the acquisition for better time management. Videos recorded in a different format (.mov or .avi) are to be converted to .tiff before analysis.

The core of our algorithm is the particle image velocimetry (PIV) calculation for which we heavily rely on the MatPIV 1.6.1 software (a GNU public license software, http://folk.uio.no/jks/matpiv/ developed by J.K. Sveen[20]) developed under MATLAB. Phase-contrast images of cells contain enough details to allow using these algorithms with no exogenous marker[10]. We have complemented the original algorithm in several ways and developed a user-friendly interface dedicated to wound-healing assays. The analysis described in the present work involves three steps that are automated and integrated in the software: (i) segmentation, (ii) velocity-field computation and (iii) edge analysis.

We first automatically determine the position of the edge of the monolayer so that the PIV is calculated on only the area covered by the cells and the computation time is kept to a minimum. To automatically identify the edge, the images of the monolayers are segmented by computing the local entropy of each image using the MATLAB entropy filter. The edge of the monolayer is the limit between the high- and low-entropy areas as defined by a single threshold whose value depends on only the cell type and illumination conditions and that remains constant during the movie. Because the direction of the physical wound is roughly prealigned with the vertical direction, this calculation is not impaired by a nonconvex boundary. The result of the calculation is then further improved with a succession of morphomathematical filters ('open', 'close' and 'dilate' (MATLAB commands imopen, imclose and imdilate)). The edge of the monolayer is easily extracted from this segmentation analysis and is chosen as the origin. From this calculation, AVeMap also extracts the free area, therefore giving access to the edge velocity and to a 'tortuosity' parameter defined as s/L, where s is the contour length of the edge and L is the distance between the two extreme points at the top and bottom boundaries of the image.

The software then computes the velocity field by PIV (**Supplementary Fig. 1**). Briefly: each single frame is divided into overlapping subwindows. Subwindow sizes (from 16 to 256 pixels)

and overlaps (from 0% to 75%) can be tuned by the user. The average displacement within a subwindow between two successive images corresponds to the position of the maximum of their cross-correlation whose calculation is performed using fast Fourier transform (FFT). Repeating this process over all the subwindows of the image yields the displacement field and hence the velocity field. At the edges, velocities are computed for subwindows whose centers are located within the monolayer after the segmentation step. This velocity field is then filtered: velocity vectors associated with a low signal-to-noise ratio are removed, and the missing vectors are interpolated by averaging the vectors associated with the neighboring subwindows. The filtering parameters can be set by the user, although the default values usually suffice.

The segmentation and PIV operations are looped over all the frames of all the movies. The parallelization of these loops over several cores of the CPU drastically reduces the computation time. For this reason, it is recommended that one use a computer equipped with a multicore processor when analyzing numerous movies (the analysis in the present report used an 8-core processor). **Supplementary Table 2** lists the range of the experimental conditions and calculation parameters compatible with AVeMap.

The results of the computation (mask and velocity field) are stored on the hard drive in the form of a matrix (one MATLAB MAT-file per movie). This way, they are available for later analysis: for instance, with AVeMap+. The software can handle a single migrating monolayer or two facing monolayers. In the case of two-facing cell sheets, the analysis is processed for each of them, and the end result is the average of this dual analysis.

Results are stored in eight distinct TXT files: V, S, $x_{V,1/2}$, $x_{S,1/2}$, a quality index ranging from 0 (meaningless) to 1 (perfect) (in practice, this parameter should be larger than 0.7; if not, the data should be reanalyzed with a different set of parameters), the area of the wound, its tortuosity and the parameters used in the calculation. In all these files, each line corresponds to a video (for example, a gene silenced, a drug, a mutant, a growth condition and so on), and columns are the time. TXT files can be easily imported into spreadsheet programs such as Microsoft Excel for further analysis.

Users interested in the full spatial profiles of the velocity and order parameter at the different times can use a second software

(AVeMap+) that generates two tables (one for V and one for S) for each selected film (lines = space; column = time) from the velocity field previously computed with AVeMap. Heat maps similar to **Figure 2d** are then easily generated from these tables with a standard graphing software.

In the present study, **Supplementary Videos 1–5** (showing HEK-HT and A549 cells) were analyzed according to the procedure described above, with the following parameters: region of interest, first 50 μm next to the border; window size, 32 pixels; overlap, 0.75; Δt, 15 min. Masking parameters for the HEK-HT cells: 0.65 (control); 0.75 (siWave2-2nM); 0.7 (siWave2-5nM). Masking parameters for the A549 cells: 0.8 (control and TGF-β).

Regarding the analysis of the MCF10A movies[2], the 67 .mov files (284×284 pixels, 200 frames each, time frame = 6 min) were first converted into TIFF files with the ImageJ plug-in QuickTime Opener (http://rsbweb.nih.gov/ij/plugins/movie-opener.html).

In this particular case, the masking steps were performed semi-manually (out of AVeMap) because of the nonconstant entropy of each movie due to the movie acquisition being in automatic gain control (AGC) mode, which is not compatible with our entropy-based calculation. The PIV analysis was then executed with the following parameters: overlap = 0.75, windowsize = 32, $\Delta t = 6$ min. The analysis for the cells at the free edge was processed over the first 30 pixels (roughly one cell size). Velocities and order parameters were averaged over either the first 10 h or the entire time of healing (when the healing lasted less than 10 h).

Statistical analysis. For the tracking experiments, velocities are first averaged out for each trajectory. The final velocity is the average of the distribution of these velocities also characterized by s.d. and s.e.m. For the AVeMap analysis, an average velocity is measured for each frame and the final velocity is the average of the distribution of these velocities also characterized by s.d. and s.e.m.

17. Hahn, W.C. *et al. Nature* **400**, 464–468 (1999).
18. Kasai, H., Allen, J.T., Mason, R.M., Kamimura, T. & Zhang, Z. *Respir. Res.* **6**, 56 (2005).
19. Rasband, W.S. ImageJ v1.46b <http://rsb.info.nih.gov/ij/> (US National Institutes of Health, Bethesda, Maryland, 1997–2012).
20. Sveen, J.K. *An introduction to MatPIV* (Mechanics and Applied Mathematics no. 2) <http://folk.uio.no/jks/matpiv/> (Department of Math, University of Oslo, 2004).